Synthesis and characterization of ball milled Fe-doped ZnO diluted magnetic semiconductor

R. Elilarassi* **and G. Chandrasekaran**

Magnetism and Nanomagnetic Materials Lab, Department of Physics, School of Physical, Chemical and Applied Sciences, Pondicherry University, Puducherry 605014, India

(Received 3 November 2011)

Fe-doped ZnO ($Zn_{0.99}Fe_{0.01}O$) powders are successfully prepared by ball milling with different milling time, and are investigated using X-ray diffraction (XRD), scanning electron microscope (SEM), ultraviolet-visible (UV-VIS) spectroscopy, vibrating sample magnetometer (VSM) and electron paramagnetic resonance (EPR) spectroscopy. The structural analysis using XRD reveals that the Fe-doped ZnO milled at different milling time can crystallize in a wurtzite structure, and in the XRD patterns, the secondary phase related to Fe cluster with the sensitivity of the XRD instrument can not be found. The SEM image of the sample milled for 24 h shows the presence of spherical nanoparticles. From the optical analysis, the optical band gap is found to decrease with increasing the milling time, which indicates the incorporation of Fe^{2+} ions into the ZnO lattice. The magnetization measurement using VSM reveals that the nanoparticles exhibit ferromagnetic behavior at room temperature, and the magnetization increases gradually with increasing the milling time. The conclusion is further confirmed by the electron paramagnetic resonance of the nanoparticles examined at room temperature, which shows an intense and broad ferromagnetic resonance signal related to Fe ions.

Document code: A **Article ID:** 1673-1905(2012)02-0109-4

DOI 10.1007/s11801-012-1157-5

In recent years, dilute magnetic semiconductors (DMSs) have been under intense research due to their potential applications in spin-based multifunctional electronic devices[1–3]. Dietl et al[4] theoretically predicted that Mn-doped ZnO and GaN could exhibit ferromagnetism above room temperature[5]. Since, for an ideal DMS material, high Curie temperature (T_C) with high magnetic moments is expected, and the essential condition must be assured that dopant atoms are uniformly dissolved into the semiconductor host lattice. Oxide diluted magnetic semiconductors (ODMSs) have high Curie temperature[5], and hence exhibit potential applications in the field of spintronic devices, such as spin field-effect transistors, spin light-emitting diodes (spin-LEDs), magneto-optical switches and spin-polarized solar cells[6-9]. Of all the ODMSs (ZnO, TiO_2, SnO_2, CeO_2), the transition metal doped ZnO has been identified as a promising host material because of its wide band gap (3.37 eV) and high exciton binding energy (60 meV). Different transition metal ions, such as Mn^{2+}[10], Ni^{2+}[11], Co^{2+}[12] and Fe^{3+} [13-15], can be doped into the ZnO lattice to tailor the material for various optical and electro-magnetic properties. Room-temperature ferromagnetism (RTFM) in ZnO:Fe system has been studied extensively in recent years[16-18], but it is still far from clear explanation on the origin of the magnetism. A wide variety of methods have been used to synthesize transition metal doped ZnO nanoparticles. But there are very few reports on the magnetic behaviour of transition metal doped ZnO synthesized using ball milling. Thus, in this paper, our aim is to synthesize ZnO:Fe ($Zn_{0.99}Fe_{0.01}O$) nanoparticles using ball milling and to study the effect of milling time on the structural, optical and magnetic properties of ZnO:Fe, which can attempt to explain the origin of ferromagnetism in these materials.

Nanocrystalline Fe-doped ZnO ($Zn_{0.99}Fe_{0.01}O$) powders were synthesized in a planetary ball mill (Fristch, Pulverisette-7, mono mill) with 10 mm diameter cemented silicon nitride balls. Starting materials are pure ZnO and FeO powder. The mixed powder was milled for different periods of time by planetary ball mill with 450 r/min. The crystal structure of the samples was examined by X-ray diffraction (XRD) analysis using a PAnalytical model X'Pert PRO XRD. The morphology of the 24 h milled $Zn_{0.99}Fe_{0.01}O$ sample was investigated using scanning electron microscope (SEM) (HITACHI Model: S-3400 N). The optical properties of the samples were analyzed using ultraviolet–visible (UV-VIS) spectrophotom-

* E-mail: ezhil1984_r@yahoo.co.uk

eter (Model:Cary 5000). Magnetic properties of the samples were experimentally studied by measuring magnetization as a function of external magnetic field using vibrating sample magnetometer (VSM) (Lakeshore 7404). Electron paramagnetic resonance (EPR) characteristics of the powder samples were studied using the JES-TE100 ESR spectrometer. The structural, optical and magnetic measurements of the samples were carried out at room temperature.

The phase purity and crystal structure of the Fe-doped ZnO ($Zn_{0.99}Fe_{0.01}O$) nanoparticles prepared using ball milling were examined by XRD. The diffraction patterns of undoped ZnO and Fe-doped ZnO milled for 8 h, 16 h and 24 h are shown in Fig.1. With the sensitivity of the XRD instrument, the diffraction peaks of all the samples indicate that the samples are in single phase with hexagonal wurtzite structure of ZnO, which is in close agreement with standard data (JCPDS file No.21-1486).

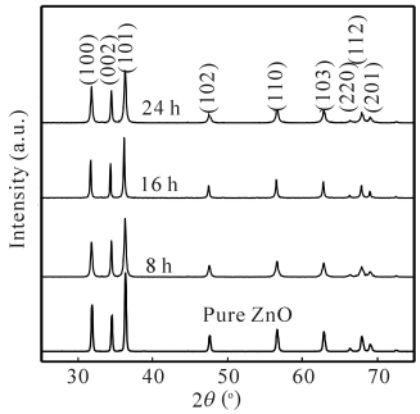

Fig.1 XRD spectra of $Zn_{0.99}Fe_{0.01}O$ nanoparticles milled for different periods of time

The XRD pattern does not show any reflection ascribed to any of the iron oxide (i.e., Fe_3O_4, Fe_2O_3, FeO, etc.) compounds for Fe-doped ZnO milled for different periods. The slight decrease in intensity and the broadening of diffraction peaks with milling time indicate that the size of nanoparticles decreases with increasing milling time.

The average crystallite size (t) of the powder samples is calculated from X-ray line broadening according to Scherrer's equation[19] using the parameters derived from the X-ray diffraction patterns

$$t = \frac{C\lambda}{\beta \cos\theta} \quad , \tag{1}$$

where t is the crystallite size (nm), $\hat{a}$ is the full width at half maximum (FWHM in radians) of (002) plane from XRD measurements, λ is the X-ray wavelength, $\grave{e}$ is the Bragg diffraction angle, and C is a correction factor which is taken as 0.9. The estimated average crystallite size in the range from 32 nm to 24 nm with increasing milling time is summarized in Tab.1. The unit cell parameters of Fe-doped ZnO nanoparticles prepared for different milling time are given in Tab.1. The observed linear decrease in the value of lattice spacing a and c with increasing milling time indicates that the structure of hexagonal-ZnO lattice gets squeezed along a and c axes. The decrease in unit cell volume reflects the overall volume contraction in the lattice of Fe-doped ZnO with increasing milling time. Such change in lattice parameters may be attributed to the incorporation of Fe atoms into the ZnO lattice. Fig.2 shows the morphology of the $Zn_{0.99}Fe_{0.01}O$ sample milled for 24 h investigated using SEM. The SEM image of the sample reveals the presence of randomly distributed spherical nanoparticles.

Tab.1 Variation of particle size and lattice parameters of Fe-doped ZnO milled for different time

Milling time (h)	Crystallite size (nm)	Lattice parameters		
		a (Å)	c (Å)	Cell V (Å)^3
8	32	3.2521	5.2117	47.73
16	29	3.2516	5.2102	47.72
24	24	3.2490	5.2051	47.58

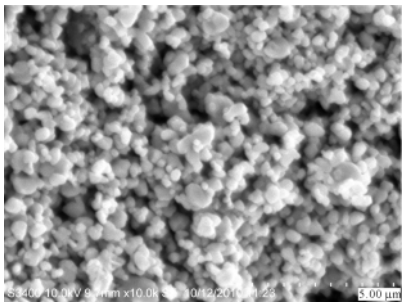

Fig.2 SEM image of $Zn_{0.99}Fe_{0.01}O$ nanoparticles milled for 24 h

The optical absorption properties of undoped and $Zn_{0.99}Fe_{0.01}O$ samples milled for different time are analyzed using UV-VIS-near-infrared (UV-VIS-NIR) spectroscopy. In Fig.3, the absorption edge of the Fe-doped samples shifts towards higher wavelength (lower energy) with increasing milling time compared with undoped ZnO. It is an indication of incorporation of Fe^{2+} ions in the ZnO lattice. Compared with the absorption spectra of pure ZnO, it could be easily confirmed that the introduction of Fe^{2+} ions into the ZnO leads to the appearance of additional absorption peak in the Fe-doped samples.

The optical band gap of the nanoparticles is determined by fitting the Tauc model[20] and the Davis and Mott model[21] in the high absorbance region as

$$(ah\upsilon)^2 = D(h\upsilon - E_g) \quad , \tag{2}$$

where $h\nu$ is the photon energy, E_g is the optical band gap, and D is a constant. For a direct transition, the square form of $ah\nu$ is chosen, since it gives the best linear fitting curve in the band edge region. The relationship between $(ah\nu)^2$ and $h\nu$ is shown in Fig.4. The values of E_g are estimated by extrapolating the vertical line portion to cut the photon energy axis in Fig.4. From Tab.2, it is found that the band gap of Fe-doped ZnO decreases with increasing milling time from that of pure ZnO. It is reported that in transitionmetal doped II-VI semiconductors, the decrease in optical band gap may be attributed to the sp-d spin-exchange interactions between the band electrons and the localized d electrons of the transitionmetal ion substituting the cation[22,23]. K. Ando et al[24] confirmed experimentally such a red shift of the band gap in co-doped ZnO. Thus, in our samples, the s-d and p-d exchange interactions between the band electrons of ZnO and localized d electrons of Fe give rise to change in the energy band structure, respectively, which can reduce the band gap.

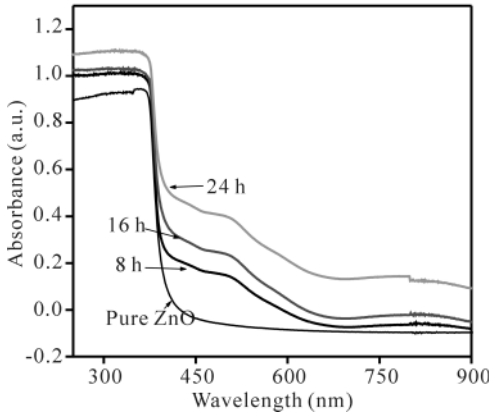

Fig.3 Optical absorption spectra of $Zn_{0.99}Fe_{0.01}O$ nanoparticles milled for different time

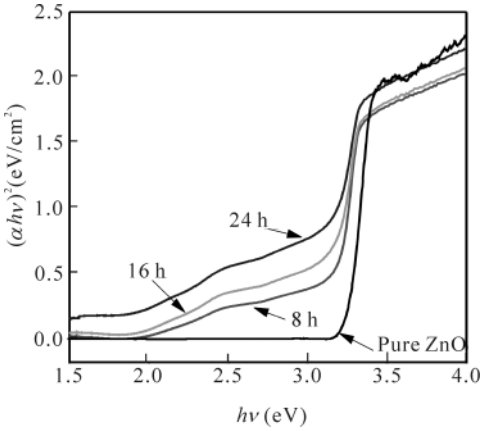

Fig.4 $(\alpha h\nu)^2$ versus $h\nu$ of $Zn_{0.99}Fe_{0.01}O$ nanoparticles milled for different time

Tab.2 Variation of optical band gap of undoped and $Zn_{0.99}Fe_{0.01}O$ samples ball-milled for different time

Samples	Band gap (eV)
Pure ZnO	3.25
$Zn_{0.99}Fe_{0.01}O$ (milled for 8 h)	3.17
$Zn_{0.99}Fe_{0.01}O$ (milled for 16 h)	3.10
$Zn_{0.99}Fe_{0.01}O$ (milled for 24 h)	3.05

Fig.5 shows magnetic hysteresis (M–H) curves of the nanoparticles measured at room temperature. The M-H measurements confirm the presence of ferromagnetism in the samples at room temperature. The ferromagnetic hysteresis loop is clearly observed from the M–H curves, and the saturation magnetization of the samples milled for 8 h, 16 h and 24 h is 0.005 emu/g, 0.020 emu/g and 0.035 emu/g, respectively. The ferromagnetism of the nanoparticles could arise from a number of possible sources. It is well known that pure ZnO is paramagnetic in nature so the observed ferromagnetism of the $Zn_{0.99}Fe_{0.01}O$ samples milled for different time may be due to Fe-doping. In general, the origin of ferromagnetism in transition metal doped semiconductors may be due to the secondary phase formation or the intrinsic property of the material. But the XRD results of the $Zn_{0.99}Fe_{0.01}O$ nanoparticles suggest that Fe is incorporated into the lattice structure with the sensitivity of XRD instrument. Thus, the possibility of ferromagnetism due to the secondary phases related to Fe cluster, such as FeO, Fe and Fe_2O_3, in the samples could be ruled out. Hence, the obtained ferromagnetism is an intrinsic magnetic property of the $Zn_{0.99}Fe_{0.01}O$ nanoparticles. It is evident from the XRD analysis that Fe is incorporated into the ZnO lattice. In addition, the absorption spectra results confirm that Fe^{2+} ions are successfully incorporated into the wurtzite lattice at the Zn^{2+} sites. In view of

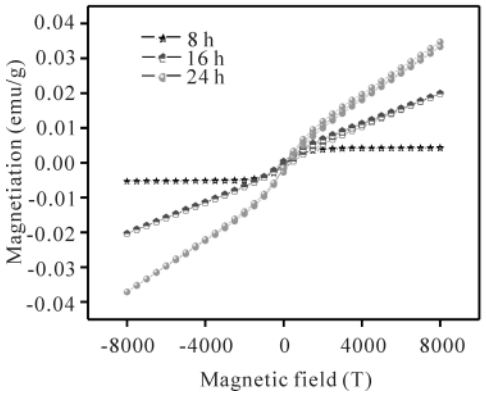

Fig.5 M–H curves of $Zn_{0.99}Fe_{0.01}O$ nanoparticles milled for different time

the Fe^{2+} ions substituted into ZnO lattice, the origin of magnetism in the samples is due to the exchange interaction between local spin-polarized electrons (such as the electrons of Fe^{2+} ions) and the conductive electrons. Such interaction can lead to the spin polarization of conductive electrons. Consequently, the spin-polarized conductive electrons undergo an exchange interaction with local spin-polarized electrons of other Fe^{2+} ions. Thus, after a successive long-range exchange interaction, almost all Fe^{2+} ions exhibit the same spin direction, resulting in the ferromagnetism of the material.

Fig.6 shows the EPR spectra of $Zn_{0.99}Fe_{0.01}O$ samples milled for different time at room temperature, including a broad and intense signal. The effective *g* factor for the broad signal is observed to be greater than 2, which clearly indicates the presence of ferromagnetism in all the samples. The resonance field (the line position) increases with increasing milling time, which is the evidence for the increase of magnetization in the samples. The observation of ferromagnetic resonance signal at room temperature and the presence of hysteresis loops provide evidence that $Zn_{0.99}Fe_{0.01}O$ nanoparticles are ferromagnetic.

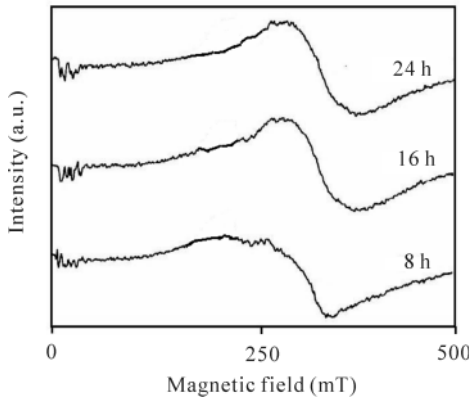

Fig.6 EPR spectra of $Zn_{0.99}Fe_{0.01}O$ milled for different time

In summary, $Zn_{0.99}Fe_{0.01}O$ diluted magnetic semiconductor nanoparticles are synthesized by ball milling and investigated using XRD, FTIR, VSM and EPR. Magnetic measurements indicate that $Zn_{0.99}Fe_{0.01}O$ is ferromagnetic at room temperature. Considering the structural, optical and magnetic studies together, we believe that the Fe element incorporated into the zinc oxide lattice by substituting the zinc atoms will result in an intrinsic ferromagnetism in the nanoparticles. The current synthetic method can be extended to the large-scale production of other transition metal doped zinc oxide nanoparticles.

References

[1] Ohno H, Science **281**, 951 (1998).
[2] Zutic I, Fabian J and Das Sarma S, Rev. Mod. Phys. **76**, 323 (2004).
[3] Furdyna J K, J. Appl. Phys. **64**, R29 (1988).
[4] Dietl T, Ohno H, Matsukura F, Cibert J and Ferrand D, Science **287**, 1019 (2000).
[5] Gould C, Slobodskyy A, Slobodskyy T, Grabs P, Becker C R, Schmidt G and Molenkamp L W, Phys. Status Solidi B **241**, 700 (2004) .
[6] Sarma S D, Nat. Matters **2**, 292 (2003).
[7] Jonker B T, Park Y D, Bennett B R, Cheong H D, Kioseoglou G and Petrou A, Phys. Rev. B **62**, 8180 (2000).
[8] Didosyan Y S, Hauser H, Reider G A and Toriser W, J. Appl. Phys. **95**, 7339 (2004).
[9] Zutic I, Fabian J and Das Sarama S, Phys. Rev. B **64**, 121201 (2001).
[10] Deka S and Joy P A, Solid State Commun. **142**, 190 (2007).
[11] Liu E, Xiao P, Chen J S, Lim B C and Li L, Curr. Appl. Phys. **8**, 408 (2008).
[12] Kim K J and Park Y R, Appl. Phys. Lett. **81**, 1420 (2002).
[13] Baek S, Song J and Lim S, Physica B **399**, 101 (2007).
[14] Chen A J, Wu X M, Sha Z D, Zhug L J and Meng Y D, J. Phys.D: Appl. Phys. **39**, 4762 (2006).
[15] Wang Y Q, Yuan S L, Liu L, Li P, Lan X X, Tian Z M, He J H and Yin S Y, Magn. Magn, Mater. **320**, 1423 (2008).
[16] Shim J H, Hwang T, Lee S, Park J H, Han S J and Jeong Y H, Appl. Phys. Lett. **86**, 082503/1 (2005).
[17] Singhal A, Achary S N, Tyagi A K, Manna P K and Yusuf S M, Materials Science and Engineering B **153**, 47 (2008).
[18] Venkatesan M, Fitzgerald C B, Lunney J G and Coey J M D, Phys. Rev. Lett. **93**, 177206 (2004).
[19] Cullity B D, Elements of X-ray Diffraction, Massachusetts: Addison Wesley Publishing Company, 1965.
[20] Tauc J, Amorphous and Liquid Semiconductors, London: Plenum, 1974.
[21] David E A and Mott N F, Philos. Mag. **22**, 903 (1970).
[22] Bylsma R B, Becker W M, Kossut J, Debska U and Yoder-Short D, Phys. Rev. B **33**, 8207 (1986).
[23] Diouri J, Lascaray J and Amrani M. El, Phys. Rev. B **31**, 7995 (1985).
[24] Ando K, Saito H, Jin Z, Fukumra T, Kawasaki M and Matsumoto Y, Appl. Phys. Lett. **78**, 2700 (2001).